J. ENVIRON. SCI. HEALTH, A36(10), 2069–2082 (2001)

SYNERGIC DEGRADATION OF REACTIVE BRILLIANT RED X-3B USING THREE DIMENSION ELECTRODE-PHOTOCATALYTIC REACTOR

TaiCheng An,* XiHai Zhu, and Ya Xiong*

School of Chemistry and Chemical Engineering,
Zhongshan University, Guangzhou, 510275, P.R. China

ABSTRACT

A new reactor, three dimension electrode-photocatalytic reactor, was designed and used to investigate the photoelectrochemical degradation of reactive brilliant red X-3B (RBRX) in simulated wastewater. The reactor was characterized by a series of parameters, the current change, decolorization ratio, COD removal and degradation ratio. It was found that the three dimensional electrode-photocatalytic reactor could effectively destroy the RBRX within a reaction time of 30 min. The results also showed that the photoelectrochemical process is more efficient than the single application of electrochemical oxidation or photocatalytic degradation. The degradation reactions of RBRX conformed to pseudo first order kinetics in the three processes, and an apparent synergic effect in the increase of the photocurrent and the disappearance of RBRX was observed by combining the electrochemistry with photocatalytic process in the three dimension electrode-photocatalytic reactor.

Key Words: Three dimensional electrode-photocatalytic reactor; Photoelectrochemical degradation; COD removal; Reactive brilliant red X-3B; Synergic effect; Wastewater treatment

*Corresponding authors. E-mail: cedc18@zsu.edu.cn.

INTRODUCTION

Photocatalytic oxidation of organic pollutants using TiO_2 as a photocatalyst has been investigated extensively in the slurry cell and immobilized-film reactor (1–2). However, the development of a practical water treatment system relative to the photocatalytic oxidation has not yet been successfully achieved (3). The high degree of recombination of photogenerated-electron and -hole is a major limiting factor controlling its photocatalytic efficiency and impeding the practical application of this technique in the degradation of contaminants in water. Recently, the following two methods have been frequently used to enhance the photocatalytic efficiency of TiO_2 for degrading undesirable organic. One of them is that using external O_2 captures the photogenerated electrons (4); another is electrochemically-assisted photocatalysis (5–7). The main purpose of the latter is to represent a proof-of-concept that anodic bias on TiO_2 electrode can drive away the photogenerated-electron and -hole in different directions, and reduce their recombination. Therefore, in the most of electrochemically assisted photocatalytic experiments, the applied anodic bias potential is almost controlled to be lower than the oxidation potential of the investigated organic pollutant so that no direct electrochemical oxidation interferes with the photocatalysis (8–9). To date, the electro-assisted photocatalysis at higher voltage has almost not been investigated.

However, it is worth to notice that recently the interest in the application of direct and/or indirect electrochemical oxidation to the treatment of the effluents from industrial or municipal plants has increased (10). In particular, the electrochemical technologies based on three-dimensional electrodes for wastewater treatment have attracted much more attention (11–13) because the electrodes are characterized with large specific surface areas and high performance in comparison to conventional two-dimensional electrode (10). However, most of researches about the three dimensional electrodes are mainly focused on organic electrosynthesis and removal of metal ions from wastewater streams (11). Recently, we have started to investigate a novel hybrid technology of organic wastewater treatment based on three dimensional electrode-slurry photocatalytic reactor. Hopefully it will be characterized by the combination of photocatalysis with electro-assisted photocatalysis and electrochemical oxidation of three-dimensional electrodes for organic pollutants. The aim of the present paper is to test primarily the degradation of organic pollutants and photoelectrochemical synergic effect in a wider range of cell voltage in a new reactor, three dimension electrode-slurry photocatalytic reactor, using Reactive Brilliant Red X-3B as a model pollutant.

EXPERIMENTAL

Material

The photocatalyst used was titanium dioxide (Degussa P25). The dye, reactive brilliant red X-3B, was reagent grade, and the dye solutions were prepared with deionized water to a concentration of 1.0 mmol·L^{-1} (COD: 265.9 ppm) without adjusting the pH of the solution. The granulated activated carbon (GAC) was used as the filler of three dimensional electrode in this experiment. It has a surface area of 870.0 $m^2 \cdot g^{-1}$, an average particle size of 3.5×5.1 mm and ash content of 8.1%. Both the main electrodes were made of stainless steel and used after certain disposition treatment.

Apparatus

Absorption spectra of reactive brilliant red X-3B were recorded with a mode UV-PC2501 spectrophotometer (Hitachi, Japan). A 500 W high-pressure mercury lamp was used as illuminant. A CHI650A electrochemical computerized system was used as a potentiostat and also was applied to determine the current in the experimental.

Photoelectrochemical Reactor

The experimental set-up is presented in Figure 1. It was an open double-layered reactor (28.0 cm × 6.0 cm × 10.0 cm) made of polytetrafluoroethylene plate. The stainless steel anode and cathode (main electrode) were equipped across the reactor. 200.0 g GAC used as particle electrodes were packed between the two main electrodes situated 26.6 cm apart from each other and the suspension of RBRX containing 1.0 g titanium dioxide was added into the reactor. When the compressed air was surged into the reactor by a micropore plate from the bottom of reactor cell, the reactors appear two layers. The upper one was mainly the suspension of TiO_2 with a height of about1.0 cm, and the down one was mainly the GAC particle electrode with a packed height of about 1.0 cm. A 500 W high-pressure mercury lamp was located 12.0 cm above the reactor as an illuminant. The emitting radiation of the illuminant are a continuous spectra in the range of 200 – 800 nm with a highest peak at 365 nm. The intensity of ultraviolet light on the surface of reaction solution was achieved at the average of 6.64 mW·cm^{-2}.

Recommended Procedure

1.0 g titanium dioxide and 200.0 mL solution of 1.0 mmol·L^{-1} reactive brilliant red X-3B was added into the reactor after the residual water for the

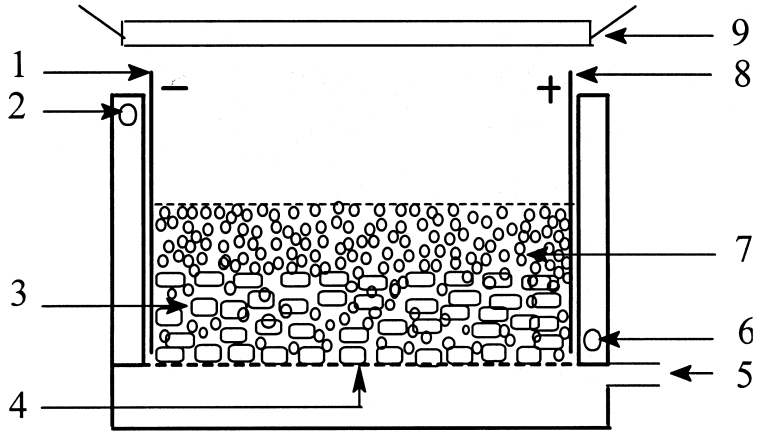

Figure 1. Schematic diagram of three dimensional electrode-photocatalytic reactor. 1-Cathode; 2-Outlet of recycled water; 3-GAC layer; 4-Micropore plate; 5-Inlet of pressured air; 6-Inlet of recycled water; 7-Titanium dioxide layer; 8-Anode; 9-UV illuminant.

clean was removed. With a 0.6 $L \cdot min^{-1}$ sparged air, certain amount of direct current and illumination, the photoelectrochemical procedure was carried out for 30.0 min in the reactor. The experimental temperature was kept at $30 \pm 2^{\circ}C$ and overheating of the reaction solution was prevented with the use of a cooling fan over the reactor. The colloid solutions were sampled at each 5 min interval, separated with centrifuge and filtered through a Millipore (0.45 um) membrane for color, degradation kinetics and COD analysis. Color and decolorization ratios were measured and calculated according to literature methods using spectrophotometer method (14–15). The analytic wavelength selected for optical absorption measurements of reactive brilliant red X-3B was 532 nm. COD was measured with potassium dichromate after the filtered sample was digested with a WMX COD microwave digestion system.

RESULTS AND DISCUSSION

Current-Voltage Characteristics

The magnitude of the photocurrent of the cell is one of major parameters characterizing photoreactor. Thus, the photocurrent was extensively investigated in the electrochemically assisted photocatalytic process. Kraeutler and Bard (16) first recognized that semiconductor particulate in the slurry cell might have similar performance with film electrode in the photoelectrochemical cell. They and other researchers have studied in detail the photocurrent -voltage curves for slurry electrode, and found that

the photocurrent is very small and lower than 0.2 μA (17), although the slurry electrode has the great advantage of good mass-transfer. Thus, a great attention has been focused, in recent years, on the investigation of semiconductor thin film reactor (18–19). The photocurrent of the thin film reactor is much higher than that of the slurry reactor and no less than 25 μA (18–20).

In our experiment, a high photocurrent, about 12.6 μA, was observed in the three dimensional electrode-slurry photocatalytic reactor, and the photocurrent is about 60 folds more than that of the reported slurry reactor (17), although it is lower than that of the mentioned-above thin film reactor. This can be considered as an enhancement effect of three dimensional electrode to slurry photocatalytic reactor. The enhancement effect can be attributed to that the three-dimensional electrode with expanded specific area has a great collecting area of photo-generated electron. It is expected that the reactor have high treatment efficiency for pollutants because the magnitude of the photocurrent of the cell is an indicator of the rate of oxidation at the anode (20).

The change of the current with cell voltage in the three dimensional electrode-photocatalytic reactor was also measured, and the current-voltage profile was shown in Figure 2. Seen from Figure 2, both current of photoelectrochemical and electrochemical process increased significantly with increase of the applied voltage. Furthermore, the current difference of the photoelectrochemical and the electrochemical process also increased as the increase of the voltage as shown in the inset of Figure 2. For example, the current difference is 19.81 μA and 68.5 μA respectively at 0.3 V and 1.0 V.

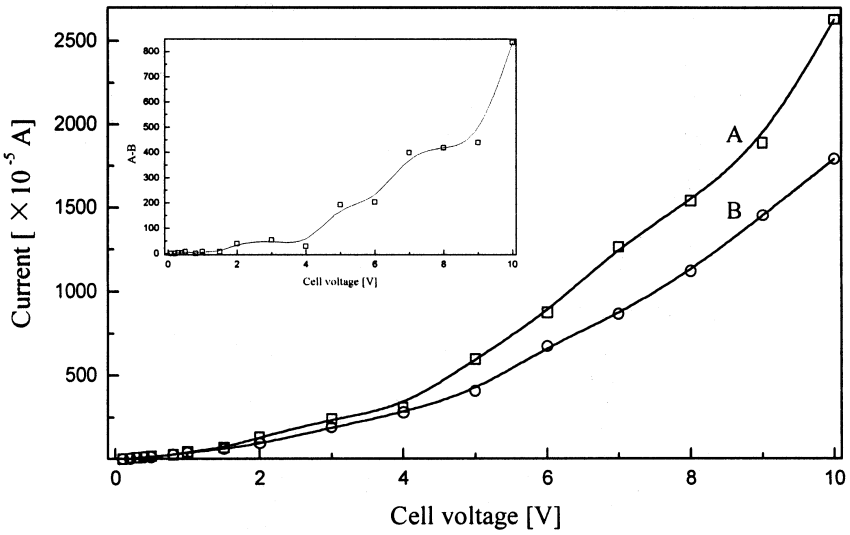

Figure 2. Dependence of current at 10 second on voltage. A-Current in the electrochemical process; B-Current in the photoelctrochemical process.

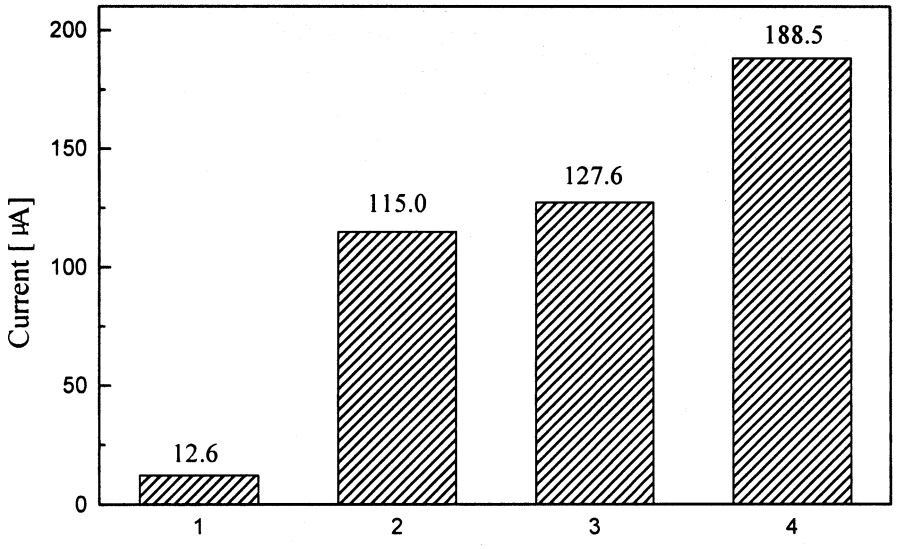

Figure 3. Comparison of current at 10 second in the various processes. 1-Photocurrent; 2-Current in the electrochemical process at 0.5 V; 3-Sum of electrocurrent at 0.5 V and photocurrent; 4-Current in the photoelectrochemical process at 0.5 V.

This result indicated that the higher the applied voltage, the stronger the ability of capturing photogenerated electron of the anode.

Additionally, it was found that the current of photoelectrochemical process was not only greater than the current of photocatalytic or electrochemical process alone, respectively, but also greater than the sum of both current of photocatalytic and electrochemical process alone. For example, for a 0.5 V of applied voltage, the current of photoelectrochemical process is 188.5 μA, while the sum of both current of photocatalytic and electrochemical process alone is only 127.6 μA, as shown in Figure 3, which is 60.9 μA lower than the former. This is a clear evidence of a synergic effect between photochemical and electrochemical process in the reactor.

Treatment Efficiency of Various Processes

The UV spectra of RBRX at various treatment conditions were presented in Figure 4. It can be observed from the figure that the absorption peaks for single photocatalytsis, single electrochemical oxidation or photoelectrochemical degradation all decreased obviously, and the curve D is much lower than others. At 532 nm, the absorption of curve D is only 4.2% of curve B and 5.6% of curve C, respectively. These changes of UV spectra indicate that the degradation of RBRX with the photoelectrochemical process have

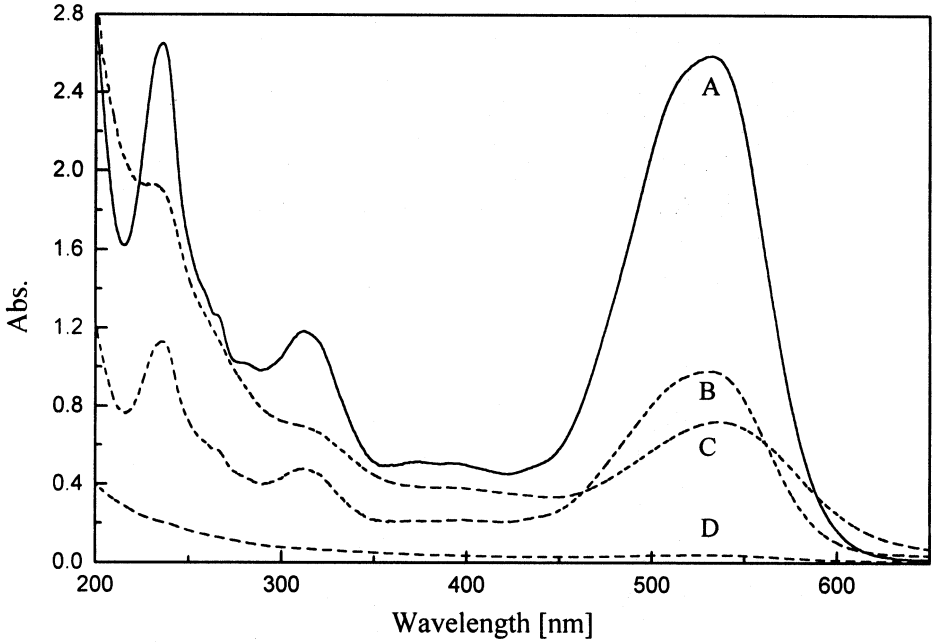

Figure 4. UV-spectra comparison of RBRX with 5-fold dilution in various conditions. A-Initial sample; B-Electrochemical treatment for 0.5 V and 30 min; C-Photocatalysis for 30 min; D-Photoelectrochemical treatment for 0.5 V and 30 min.

more efficient than the photocatalytic and electrochemical process alone. Moreover, the COD removal efficiencies for various processes can further confirm the view. When no voltage and no illumination was applied, only a 27.1% of COD removal was observed with 30.0 min, which is attributed to the adsorption of TiO_2 and GAC. When a 30.0 V of cell voltage or illumination was applied alone, the COD removal increased to 53.6% and 58.6%, respectively. These COD removal efficiencies were apparently lower than that of photoelectrochemical process (77.3%). This enhancement effect of COD removal of photoelectrochemical process may be also an evidence of photoelectrochemical synergic effect which exists in the three dimensional electrode-photocatalytic reactor.

Effect of the Applied Cell Voltage

The effect of applied voltage on the decolorization ratios was conducted and the profile was shown in Figure 5. In the profile, it is obvious that both decolorization ratios in the electrochemical and photoelectrochemical processes increased sharply in all range of cell voltage from 0 V to 30 V, however, the decolorization of the latter is always higher than that of the former.

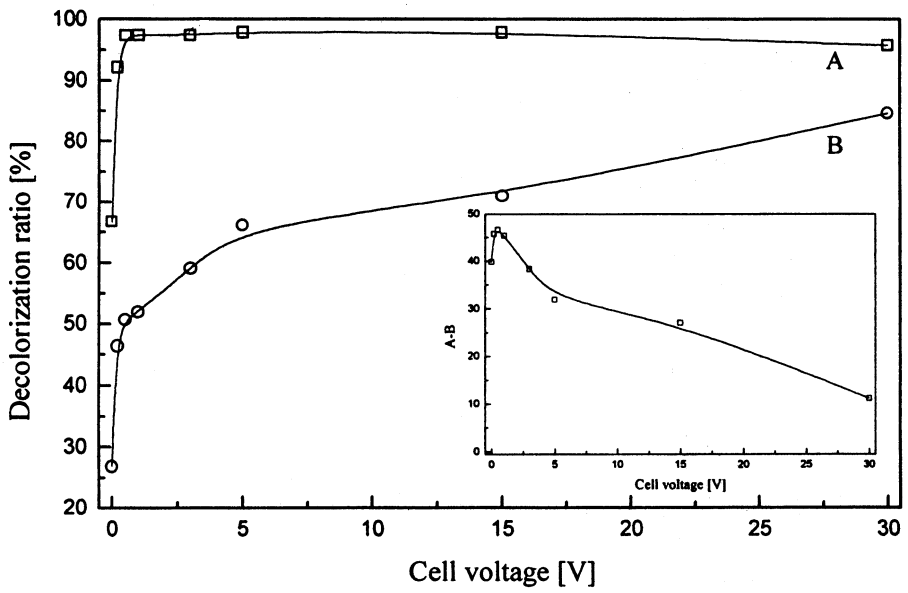

Figure 5. Effect of cell voltage on decolorization ratio. A-Decolorization ratio in the photoelectrochemical process; B-Decolorization ratio in the electrochemical process.

Furthermore, the difference of their decolorization ratio is also dependent on the applied voltage. As shown in the inset of Figure 5, when the voltage is lower than 0.5 V, the difference increased with the increase of voltage. When the voltage is higher than 0.5 V, the difference decreased with the increase of voltage, leading apparently to a maximum at 0.5 V.

The role of potential bias in the photocatalytic degradation of organic pollutants is not only limited to reducing the electron-hole recombination, but also can still have a direct or/and indirect electrochemical oxidation to the organic pollutant. Thus, we could see from the curve B of Figure 5 that the decolorzation ratio of electrochemical effect increased dramatically than that of photoelectrochemistry at the high cell voltage. It means that the electrochemical oxidation of the dyes is the predominated reaction in the photoelectrochemical process at these voltages. A similar conclusion could also be reached by considering the reduction of COD. As shown in Figure 6, both curves increased dramatically with the increase of cell voltage and changed gradually beyond 5.0V. It is worth to notice that at the lower voltage, the differences of two curves are greater. It means that there is a more significant synergic effect existing in the photoelectrochemical process at lower voltage than at the higher voltage. The synergic effect at the lower voltage may origin from the reduction of photo-generated electrons and hole, not from other reactions because no any electrochemical reaction occurs at the lower voltage.

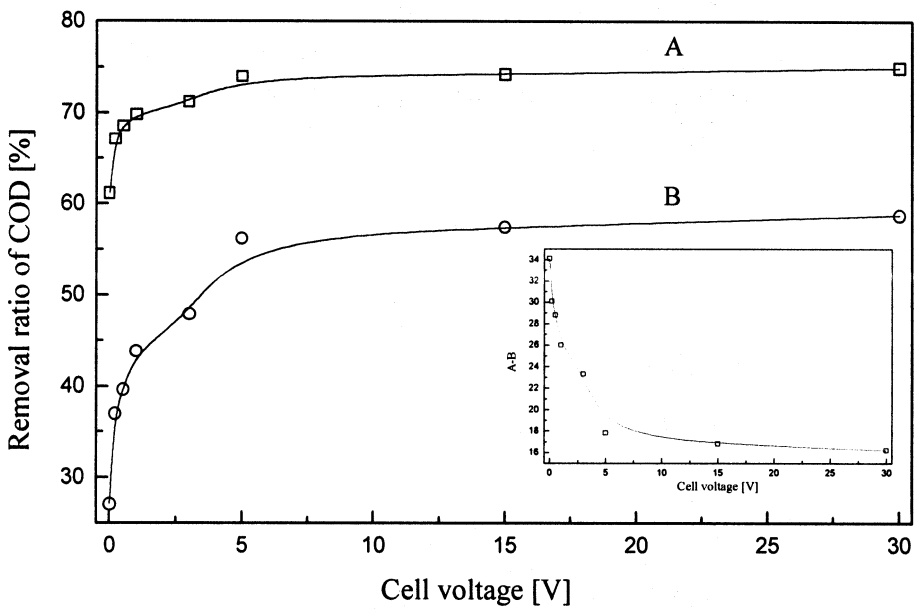

Figure 6. Effect of cell voltage on COD removal. A-COD removal in the photoelectrochemical process; B-COD removal in the electrochemical process.

Although the differences in current of single electrochemical process and photoelectrochemical process decreased with the cell voltage, as shown in the inset of Figure 2, the difference in COD removal of both the process decreased with increase of cell voltage. The discrepancy of these difference changes is mainly due to the enhanced current in photoelectrochemical process is not contributed completely to the COD removal.

Synergic Degradation Kinetics

The changes of UV spectra of RBRX in the photoelectrochemical process at various reaction intervals were investigated and presented in Figure 7. It could be observed that RBRX decreased dramatically and the shape of spectra was also changed greatly as reaction time increased. The significant decrease and changes in the ultraviolet as well as visible region can reflect that most of RBRX was completely mineralized with prolong of the reaction.

The photocatalytic degradation, electrochemical oxidation and the photoelectrochemical degradation of RBRX all accord with apparent pseudo first-order kinetics, and the kinetic regression equations and parameters of all reactions are listed in Table 1, respectively. The apparent rate constant for photocatalytic and photoelectrochemical process respectively equal to 0.0351

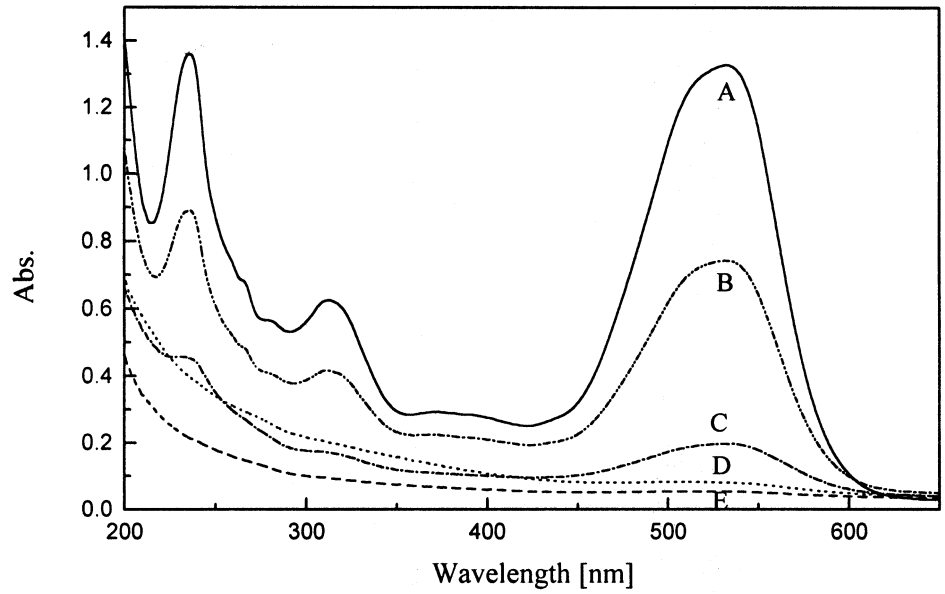

Figure 7. Absorption spectra of RBRX with 10-fold dilution at various treating time. A-0 min; B-5min; C-10 min; D-20 min; E-30 min.

Table 1. Kinetic Regression Equations and Parameters in Various Processes

Processes	Kinetic Regression Equations	Regression Coefficient	Kinetic Constant (min^{-1})	Half Life (min)
Illumination and voltage	A = 0.0746–0.1067t	0.990	0.1067	6.5
Only illumination	A = 0.3646–0.0351t	0.999	0.0351	19.7
Only voltage	A = 0.2662–0.0562t	0.982	0.0562	12.3

and 0.1067 min^{-1}. The rate constant of the latter is 2.94 folds of the former. The increase indicates that an apparent synergic effect in the disappearance of RBRX was obtained in the three dimensional electrode-slurry photocatalytic reactor (21).

Reaction Mechanism

The reaction mechanisms for the single application of photocatalytic oxidation have been convincingly studied and reported in the literature (1). Many researchers (22–23) have also studied the reaction mechanisms of electrochemical process with GAC electrodes. All believed that oxygen could be

changed into the stronger oxidizing agent, H_2O_2, on the electrode by a two-electron reduction of oxygen. The electrogenerated H_2O_2 can be further changed into the OH· radical, in situ, by photolysis reaction in the presence of UV light in the three dimensional electrode-photocatalytic reactor (24). Thus, one of the degradation mechanisms of organic pollutants in the reactor is convinced to be the OH·oxidation besides anodic oxidation. It is also believed that the reaction of the photoeletro-generated OH·radical, in situ, is an important origin of the mentioned-above synergic effect of the COD removal besides the recombining reduction of photogenerated- electron and -hole by anodic bias.

In addition, it is well known that a large amount of water must be electrolyzed in the reactor with the generation of oxygen and hydrogen at electrodes, besides the direct and indirect electrochemical oxidation of the organic compounds (10, 23) when a 30 V DC was acted across the three dimensional electrodes. The side reaction on the reactor may have occurred, as below: $H_2O \rightarrow 1/2\ O_2 + H_2$.

It is worth to notice that the oxygen can be used as a photo-generated electron scavenger, enhancing the photocatalytic efficiency (25), which is another origin of the above-mentioned synergic effect of the COD removal in the reactor. Moreover, OH· can be generated at the anode surface at the same time of oxygen evolution (10, 26–27). These agents generated, in situ, can also cause the oxidation of RBRX and its intermediates. Thus, in the paper, the major photoeletrochemical reactions initiating redox processes in the photoelectrochemical reactor can be summarized as follows (7, 22–23, 26–27):

$$\text{Anode} + \text{dye} \rightarrow \text{Products} \tag{1}$$

$$2H_2O - 2e \rightarrow 2OH\cdot + 2H^+ \tag{2}$$

$$\text{Cathode(e)} + O_2 \rightarrow O \tag{3}$$

$$O + e + 2H^+ \rightarrow H_2O_2 \tag{4}$$

$$TiO_2 + h\nu \rightarrow TiO_2(h \ldots \nu) \tag{5}$$

$$TiO_2(h) + \text{dye} \rightarrow TiO_2 + \text{Products} \tag{6}$$

$$TiO_2(h) + OH^- \rightarrow TiO_2 + OH\cdot \tag{7}$$

$$H_2O_2 + h\nu \rightarrow 2OH\cdot \tag{8}$$

$$OH\cdot + \text{dye} \rightarrow \text{Products} \tag{9}$$

Where e and h are the electron and hole, respectively, which are formed within the semiconductor particles after bandgap excitation. From the above-mentioned mechanisms, the degradation of dye can be carried out by many oxidation routines, such as anodic oxidation, the oxidation of electrogenerated H_2O_2 and OH·, the oxidation of photogenerated hole and OH·, and the photoelectrochemical synergic effect etc. This may be a good

interpretation of effective destroying of RBRX using the three dimensional electrode-slurry photocatalytic reactor.

CONCLUSIONS

An apparent synergic effect of RBRX degradation was confirmed by a series of parameters, the current change, decolorization ratio, COD removal and degradation ratio in a new designed reactor, three dimension electrode-photocatalytic reactor. Moreover, it was found that the reactor could more efficiently destroy the RBRX than the single application of electrochemical oxidation or photocatalytic degradation within a reaction time of 30 min. It is expected that the photoelectrochemical process based on the reactor is a promising technology for removing organic pollutants from wastewater.

ACKNOWLEDGMENTS

Financial support by NSF of China (29977030), NSF of Guangdong Province, China (990274 & 970167), R.& D. Project of EPA of Guangdong province, China (1999-14) and Univ. Key laboratory of Environ. Sci. & Tech. of Henan province.

REFERENCES

1. Hoffmann, M.R.; Martin, S.T.; Choi, W. Environmental Application of Semiconductor Photocatalysis. Chem. Rev. **1995**, *95*, 69–96.
2. Legrini, O.; Oliveros, E.; Braun, A.M. Photochemical Processes for Water Treatment. Chem. Rev. **1993**, *93*, 671–698.
3. Ray, A.K.; Beenackes, A.A. Development of A New Photocatalytic Reactor for Water Purification. Catal. Today. 1998, *40*, 73–83.
4. Hung, G.H.; Marinas, B.J. Role of Chlorine and Oxygen in the Photocatalytic Degradation of Trichoroethylene Vapor on TiO_2 Film. Environ. Sci. Technol. **1997**, *31*, 562–568.
5. An, T.C.; Zhu, X.H.; Xiong, Y. Feasibility Study of Photoelectrochemical Degradation of Methylene Blue with Three Dimensional Electrode-Photocatalytic Reactor, Chemosphere, 2001, Accepted.
6. Kesselman, J.M.; Lewis, N.S.; Hoffmann, M.R. Photoelectrochemical Degradation of 4-Chlorocatechol at TiO_2 Electrodes: Comparison Between Sorption and Photoreactivity. Environ. Sci. Technol. **1997**, *31*(8), 2298–2302.
7. Peterson, M.W.; Turner, J.A.; Nozik, A.J. Mechanistic Studies of the Photocatalytic Behavior Of Titania: Particles in A Photoelectrochemical Slurry Cell and the Relevance to Photodetoxification Reactions. J. Phys. Chem. **1991**, *95*(1), 221–225.z

8. Butterfield, I.M.; Christensen, P.A.; Hamnett, A.; Shaw, K.E.; Walker, G.M.; Walker, S.A.; Howarth, C.R. Applied Studies on Immoblilized Titanium Dioxide Films As Catalysts for The Photoelectrochemical Detoxification of Water. J. Appl. Electrochem. **1997**, *27*(4), 385–395.
9. Byrne, J.A.; Eggins, B.R.; Byers, W.; Brown, N.M.D. Photoelectrochemical Cell for the Combined Photocatalytic Oxidation of Organic Pollutants and the Recovery of Metals from Wastewaters. Applied Catalysis B: Environ. **1999**, *20*(2), L85–L89.
10. Brillas, E.; Sauleda, R.; Casado J. Peroxi-Coagulation of Aniline in Acidic Medium Using An Oxygen Diffusion Cathode. J. Electrochem. Soc. **1997**, *144*, 2374–2379.
11. Simonsson, D. Electrochemistry for A Cleaner Environment. Chem. Soc. Rev. **1997**, *26*(3), 181–189.
12. Xiong, Y.; Karlsson, H.T. Approch to A Two-Step Process of Dye Wastewater Containing Acid Red B. J. Environ. Sci. Health, Part A, **2001**, *36*(5), 321–331.
13. Xiong, Y.; Peter, H.; Xia, H.Y.; Zhu, X.H.; Karlsson, H.T. Treatment of Dye Wastewater Containing Acid Organge II Using A Cell with Three-Phase Three-Dimensional Electrode. Wat. Res. **2001**, in press.
14. Zhou, J.J. Spectrophotometric Determination of the Colourity of Dyeing Wastewater. Electroplating and Environmental Protection. **1988**, *8*, 39–42.
15. An, T.C.; Gao, J.Z.; Chen H.; Zhu, X.H. Heterogeneous Photocatalytic Degradation of Methylene Blue Aqueous Solution under Coexistence of Metalloporphyrin Polymer and Air. Chem. J. Internet. **2001**, *3*(4), 14.
16. Kraeutler, B.; Bard, A.J. Heterogeneous Photocatalytic Synthesis of Methane from Acetic Acid – New Kolbe Reaction Pathway. J. Am. Chem. Soc. **1978**, *100*(7), 2239–2240.
17. Bard, A.J. Photoelectrochemistry and Heterogeneous Photocatalysis at Semiconductors. J. Photochem. **1979**, *10*(1), 59–75.
18. Vinodgopal, K.; Stafford, U.; Gray, K.A.; Kamat, P.V. Electrochemically Assisted Photocatalysis. 2. The Role of Oxygen and Reaction Intermediates in the Degradation of 4-Chlorophenol on Immobilized TiO_2 Particulate Films. J. Phys. Chem. **1994**, *98*(27), 6797–6803.
19. Wahl, A.; Ulmann, M.; Carroy, A.; Augustynski, J. Highly Selective Photooxidation Reactions at Nanocrystalline TiO_2 Film Electrodes. J. Chem. Soc., Chem. Commun. 1994, *19*, 2277–2278
20. Haque, I.U.; Rusling, J.F.; Photodegradation of 4-Chlorophenol to Carbon and HCl Using High Surface Area Titanium Dioxide Anodes. Chemosphere. **1993**, *26*(7), 1301–1309.
21. Matos, J.; Laine, J.; Herrmann, J.M. Synergy Effect in the Photocatalytic Degradation of Phenol on A Suspended Mixture of Titania and Activated Carbon. Appl. Catal. B: Environ. **1998**, *18*, 281–291.
22. Alverez-Gallbergos, A.; Pletcher, D. The Removal of Low Level Organics via Hydrogen Peroxide Formed in A Veticulated Vitreous Carbon Cathode Cell. Part 2: The Removal of Phenols and Related Compounds from Aqueous Effluents. Electrochim. Acta. **1999**, *44*(14), 2483–2492.
23. Pletcher, D. Indirect Oxidations Using Electrogenerated Hydrogen Peroxide, Acta Chemica Scandinavica. **1999**, *35*, 745–750.

24. Chen, H.; An, T.C.; Fang, Y.J.; Yu, T.Z. Photocatalytic Activity Study of Co(II) Tetra–(Chloromethyl-Phenyl) Porphyrin in Oxidation Reaction of Aromatic Aldehydes. Indian J Chem. **1999**, *38B*(7), 805–809.
25. Vinodgopal, K.; Hotchandani, S.; Kamat, V. Electrochemically Assisted Photocatalysis. TiO_2 Particulate Film Electrodes for Photocatalytic Degradation of 4-Chlorophenol. J. Phys. Chem. **1993**, *97*, 9040–9044.
26. Canizares, P.; Dominguez, J.A.; Rodrigo, M.A.; Villasenor, J.; Rodriguez, J. Effect of The Current Intensity in the Electrochemical Oxidation of Aqueous Phenol Wastes at An Activated Carbon and Steel Anode. Ind. Eng. Chem. Res. **1999**, *38*, 3779–3785.
27. Comninllis, C.; Battisti, A.D. Electrocatalysis In Anodic Oxidation of Organics with Simultaneous Oxygen Evolution. J. Chim. Phys. Phys.-Chim. Biol. **1996**, *93*, 673–679.

Received April 19, 2001